広島大学学術情報リポジトリ
Hiroshima University Institutional Repository

Environmentally-Benign Synthesis and Color Tuning of Strontium–Tantalum Perovskite Oxynitride and Its Solid Solutions

Takuya Sakata,[†,‡] Risa Yoshiyuki,[†] Ryoki Okada,[†] Sohta Urushidani,[†] Naoki Tarutani,[†]
Kiyofumi Katagiri,*[,†] Kei Inumaru,[†] Kyohei Koyama,[§] and Yuji Masubuchi[‖]

[†] Graduate School of Advanced Science and Engineering, Hiroshima University, 1-4-1 Kagamiyama, Higashi-Hiroshima 739-8527, Japan

[‡] Western Region Industrial Research Center, Hiroshima Prefectural Technology Research Institute, 2-10-1 Aga-Minami, Kure 737-0004, Japan

[§] Graduate School of Chemical Sciences and Engineering, Hokkaido University, N13 W8, Kita-ku, Sapporo 060-8628, Japan

[‖] Division of Applied Chemistry, Faculty of Engineering, Hokkaido University, N13 W8, Kita-ku, Sapporo 060-8628, Japan

*E-mail: kktgr@hiroshima-u.ac.jp

ABSTRACT: A facile method was successfully developed to prepare strontium–tantalum perovskite oxynitride, $SrTaO_2N$, and its solid solutions. Urea was employed as a solid nitriding agent to eliminate the use of toxic NH_3 gas. In addition, utilization of sol-gel derived Ta_2O_5 gel as a Ta precursor allowed for completion of nitridation within a shorter period and at a lower calcination temperature compared with the conventional ammonolysis process. Optimization of the reaction conditions, such as the urea content, allowed for production of solid solutions of $SrTaO_2N$ and $Sr_{1.4}Ta_{0.6}O_{2.9}$. The products exhibited optical absorption and chromatic colors because of the narrower band gaps of oxynitrides compared with those of oxides. The O/N ratios of the solid solutions were easily adjusted by varying the amount of urea in the mixture of precursor. As a result, the colors of the products ranged from yellow to brown. The nitridation process and products developed in this study are interesting environmentally-benign alternatives to conventional inorganic pigments.

INTRODUCTION

Coloring of surfaces by colorants provides aesthetic appeal to many products used in daily life.[1,2] One of the major concerns in any industry that uses colorants is color stability against thermal and chemical degradation. Inorganic pigments are generally used in various products, such as paints, plastics, ceramics, and glasses because they have excellent thermal and chemical resistance compared with organic dyes and pigments.[3–5] Several inorganic pigments, such as cadmium red ($CdS·CdSe$), cadmium yellow ($CdS·ZnS$), cobalt blue ($CoAl_2O_3$), mercuric sulfide red (HgS), and lead chromate ($PbCrO_4$), are commonly used. However, these pigments contain toxic and polluting elements, such as Cd, Co, Hg, Pb and Cr, which are hazardous to the environment and human health.[3,6–9] Due to the high toxicity, the use of such hazardous substances becomes strictly restricted by legal regulations, e.g., the Restriction of Hazardous Substances (RoHS) directive.[10] Moreover, the Global Alliance to Eliminate Lead Paint, co-led by the World Health Organization (WHO) and the United Nations Environment Programme (UNEP), announced an international goal of eliminating lead in paints by 2020. Therefore, a great deal of effort has been put into eliminating the use of toxic heavy metals and also to produce new types of colorants, such as new inorganic pigments that are composed entirely of harmless substances.[3,11–19]

Metal oxynitrides have attracted attention in various fields for use in photocatalysts,[20–22] phosphors,[23,24] colossal magnetoresistive materials,[25] and high-κ dielectrics.[26,27] In addition, they have recently been considered as promising replacements for inorganic pigments containing toxic elements.[11,28–33] The wide bandgap of most metal oxides does not allow for visible light absorption. The band gap energy can be reduced by substituting nitrogen as an anion with less electronegativity, which pulls the upper end of valence band of oxynitrides higher than that of oxides because the N 2p state is involved in valence band formation. The resulting metal oxynitrides can absorb visible light.[31,34,35] Furthermore, the band gap energy can be controlled by varying the O/N molar ratio in oxynitrides to generate various colors. Jansen et al. reported that solid solutions of the perovskite oxynitrides $CaTaO_2N$ and $LaTaON_2$ exhibited yellow to red colors and showed potential as alternatives to pigments containing Cd.[11] In addition, Kim et al. reported that perovskite-type oxynitrides had various colours.[26] For example, $BaTaO_2N$ was red-brown, $SrTaO_2N$ was orange-red, $BaNbO_2N$ was black-brown, and $SrNbO_2N$ was dull brown. However, when considering practical application, critical obstacles still exist in the synthesis of perovskite oxynitrides. Generally, perovskite oxynitrides are synthesized with a stream of harmful NH_3 gas for long periods at high temperatures.[36–38] Usually, the heat-treatment at relatively high temperature (e.g., 1000 °C) for

long duration (e.g., 24 h) are required to complete the synthesis of oxynitrides via ammonolysis. The ammonolysis reaction conditions are high risk and it is a difficult reaction to conduct on an industrial scale. Therefore, development of a novel strategy for ammonolysis-free synthesis of metal oxynitrides is one of the most critical issues in this field.

It has been reported that metal nitrides and oxynitrides can be synthesized from metal oxide precursors with molten $NaNH_2$ salts.[39–42] Metal oxynitrides, such as $BaTaO_2N$[41] and $BaNbO_2N$,[42] have been synthesized using $NaNH_2$ as a nitriding agent. However, because $NaNH_2$ is extremely sensitive, these syntheses are difficult to scale-up. Sun and co-workers reported that the preparation method of $SrTaO_2N$ using $SrCO_3$ and Ta_3N_5 under N_2 atmosphere.[43] Solid solutions of $BaTaO_2N$ and $SrTaO_2N$ have also been synthesized using $BaCN_2$.[44,45] However, the precursors that contain nitrogen, i.e., Ta_3N_5 and $BaCN_2$, must be prepared beforehand by using NH_3 gas, meaning that these methods cannot completely eliminate the use of gaseous NH_3. Sun et al. recently reported preparation of $SrTaO_2N$ using TaN, instead of the Ta_3N_5.[46] This procedure can eliminate the use of NH_3 because TaN is commercially available and prepared by reaction of Ta metal and nitrogen, in the absence of NH_3. Preparation of metal oxynitrides through nitridation of metal oxide precursor using solid nitriding agents, such as C_3N_4 and urea, is reportedly a safe and simple method that does not use gaseous NH_3. Masubuchi et al. reported on the preparation of perovskite oxynitrides using C_3N_4.[47,48] Giordano et al. reported on the synthesis of tantalum oxynitrides and nitrides by a Ca-assisted urea method.[49] Gomathi and Rao reported preparation of various metal oxynitrides through urea-based route.[50] Both groups insisted that the thermal decomposition of urea generated NH_3 and it reacted with precursors, i.e., carbonates and oxides. This insistence is uncertain because it is unrealistic to expect that NH_3 generated from urea decomposition remains in the reaction furnace until it reaches high temperature under N_2 flow. Recently, we achieved syntheses of metal oxynitrides, such as $LaTiO_2N$[51] and GaN:ZnO solid solution[52], using urea as a nitriding agent. We elucidated the nitriding mechanisms of GaN:ZnO and $LaTiO_2N$. In these systems, the nitridation does not occur with NH_3 generated by the decomposition of urea, metal (oxy)cyanamides, such as $ZnCN_2$ and $La_2O_2CN_2$, generate as intermediates by the reaction of urea-decomposed species and metal precursors and plays important roles for nitridation. Although it is evident that the precursors are key to production of metal oxynitrides via the urea method, preparation of Ta-containing perovskite-type oxynitrides with controlled O/N contents via the urea method has not yet been reported.

The aim of the present study was to extend on the above efforts to develop a facile approach to prepare strontium–tantalum perovskite oxynitride and tune the color of its solid solution using urea as a nitriding agent. Tantalum oxide (Ta_2O_5) gel, for use as the precursor, was prepared by the sol-gel method via hydrolysis and polycondensation of tantalum ethoxide ($Ta(OC_2H_5)_5$). Compared with crystalline Ta_2O_5, we predicted that the amorphous gel state would favor the nitriding process using urea because it has a thermodynamically metastable state.[53] We examined the effects of the reaction conditions, such as the temperature of heat-treatment and molar ratio of urea in the precursor mixture. We also attempted to control the oxygen/nitrogen (O/N) ratio in the oxynitride solid solutions by varying the amount of urea. Adjusting of the O/N ratio would allow for tuning of the colors of the solid solutions.

EXPERIMENTAL PROCEDURE

Materials. Strontium carbonate ($SrCO_3$, purity ≥99.9 %) was purchased from Kishida Chemical Co., Ltd. (Osaka, Japan). Tantalum(V) ethoxide, $Ta(OC_2H_5)_5$, was obtained from Hokko Chemical Industry Co., Ltd. (Tokyo, Japan). Urea ($CO(NH_2)_2$, purity ≥99 %), ethanol (EtOH; purity ≥ 99.5%), and Ta_2O_5 were purchased from Nacalai Tesque, Inc. (Kyoto, Japan). All chemicals were used without further purification. A water purification system, Milli-Q (Merck Millipore, Billerica, MA, USA), was employed to prepare deionized water used in all experiments in this study.

Preparation of Tantalum Oxide Gel. Amorphous gel of Ta_2O_5 was synthesized from tantalum alkoxide. First, a mixture of 1 mmol of $Ta(OC_2H_5)_5$ and 1 mL of EtOH was prepared. Then, 5 mL of deionized water was added to this mixture dropwise under stirring at room temperature. The hydrolysis and condensation of $Ta(OC_2H_5)_5$ rapidly lead to precipitation of Ta_2O_5 gel after addition of water. The precipitate thus generated was collected by centrifugation and dried in an oven at 50 °C overnight.

Preparation of Strontium–Tantalum Perovskite Oxynitrides. Ta_2O_5 gel prepared as above was used as a precursor for preparation of strontium–tantalum perovskite oxynitrides. $SrCO_3$, Ta_2O_5 gel, and urea, which was employed as a solid-state nitriding agent, were mixed in an agate mortar and pestle. The molar ratio of $Sr/Ta/CO(NH_2)_2$ in this mixture ($Sr:Ta:CO(NH_2)_2 = x:y:z$) was 1:1:0, 1:1:1, 1:1:2, 1:1:3, 1:1:4, 1:1:5, or 1:1:6. The mixture was heated using an alumina crucible in a horizontal tube furnace under a flow of N_2 gas (purity 99.99 %, 300 mL min^{-1}). The heating rate of the furnace was 15 °C min^{-1}. The final heat-treatment temperature was varied from 100 °C to 900 °C. The heating period at the final heat-treatment temperature was 2 h. For comparison, commercial crystalline Ta_2O_5 was used in the same reaction instead of the alkoxide-derived Ta_2O_5 gel.

Characterizations. Structural analysis of the obtained samples has been performed using the X-Ray Diffraction (XRD; D8 Advance, Bruker AXS, Karlsruhe, Germany) using Cu-Kα radiation. Scanning electron microscopy (SEM; Hitachi, S-4800) was employed to observe the morphologies of the obtained samples. Sputter coatings of Pt were performed before SEM observations. UV-Vis diffuse reflectance spectra were measured using a V-670 spectrophotometer (JASCO, Tokyo, Japan). The band gap energies (E_g) of the products were determined by extrapolation of the absorption edge of the absorption spectra processed using the Kubelka–Munk function, $f(R) = (1 − R)^2/2R$, where R is the reflectance.[54] A chromometer (CR-300, Konica Minolta, Inc., Tokyo, Japan) was employed to evaluate $L*a*b*$ color parameters of the products in accordance with the CIE [Commission International del'Eclairage] colorimetric method. The parameter $L*$ indicates lightness (0 = black, 100 = white) and the $a*$ and $b*$ are the

chromaticity coordinates and indicate color directions: $+a*$ is the red direction, $-a*$ is the green direction, $+b*$ is the yellow direction, and $-b*$ is the blue direction. The chroma parameter (C) expresses the color saturation of the product and it can be defined by the following equation: $C = [(a*)^2 + (b*)^2]^{1/2}$. The hue angle ($h°$) can be between 0° and 360°, and is within the following ranges for different colors: red, 35°–350°; orange, 35°–70°; yellow, 70°–105°; green, 105°–195°; blue, 195°–285°; and violet, 285°–350°.[55] The value of $h°$ can be calculated using the equation $h° = tan^{-1}(b*/a*)$. The Sr and Ta contents were measured by inductively coupled plasma optical emission spectroscopy (ICP-OES) using an ICAP 6500 (Thermo Fisher Scientific, Waltham, MA USA). The O and N contents in the samples were investigated by an oxygen/nitrogen combustion analyzer (EMGA-620W, HORIBA Ltd., Kyoto, Japan).

RESULTS AND DISCUSSION

First, Ta_2O_5 gel, a precursor of strontium–tantalum perovskite oxynitrides, was prepared by hydrolysis and condensation of $Ta(OC_2H_5)_5$. Figure S1 shows the XRD patterns of Ta_2O_5 gel and commercial crystalline Ta_2O_5. In contrast to the XRD pattern of crystalline Ta_2O_5, that of the Ta_2O_5 gel displayed a broad halo pattern without any sharp diffraction peaks, which was indicative of formation of amorphous Ta_2O_5. Next, we synthesized strontium–tantalum perovskite oxynitrides using the obtained amorphous Ta_2O_5 gel. $SrCO_3$ and urea which were chosen as a Sr source and the nitriding agent, respectively. For comparison, synthesis of strontium–tantalum oxynitrides using crystalline Ta_2O_5 instead of the amorphous gel was also performed. Optical photographs and XRD patterns of the products obtained after calcination of $SrCO_3$, Ta_2O_5, and urea are shown in Figure 1. The molar ratio of $Sr/Ta/CO(NH_2)_2$ was 1:1:5. The heat-treatment temperature and period were 900 °C and 2 h, respectively. As depicted in Figure 1a, the product prepared using crystalline Ta_2O_5 was pale yellow. Although the XRD pattern of the sample exhibited broad peaks that could be assigned to $SrTaO_2N$ (ICDD PDF #79-1311), diffraction peaks for $SrTa_2O_6$ (ICDD PDF #77-0943) were also observed. By contrast, the product prepared using the Ta_2O_5 gel was red-brown, and was consistent with $SrTaO_2N$ prepared by the typical ammonolysis method.[26,31] The XRD pattern of this product showed sharp peaks for $SrTaO_2N$ and no peaks for by-products. These results show that the Ta_2O_5 gel obtained by hydrolysis and condensation of $Ta(OC_2H_5)_5$ is a much more suitable precursor for $SrTaO_2N$ in the urea nitriding process than crystalline Ta_2O_5. Therefore, Ta_2O_5 gel was used for subsequent experiments.

We optimized the reaction temperature for preparation of $SrTaO_2N$ using urea. The XRD patterns of the products obtained from mixtures of $SrCO_3$, Ta_2O_5 gel, and urea after calcination at 100 °C, 300 °C, 500 °C, 700 °C, 800 °C, and 900 °C are shown in Figure 2. The calcination period was 2 h. The molar ratio of $Sr/Ta/CO(NH_2)_2$ in the starting mixture was 1:1:5. When the mixture was heat treated at 100 °C, the XRD pattern of the product contained peaks for $SrCO_3$ and urea and no other peaks were observed. It is unlikely that the urea decomposed at 100 °C because its decomposition temperature is about 140 °C.[56] When the mixture was heat-treated at 300 °C, only
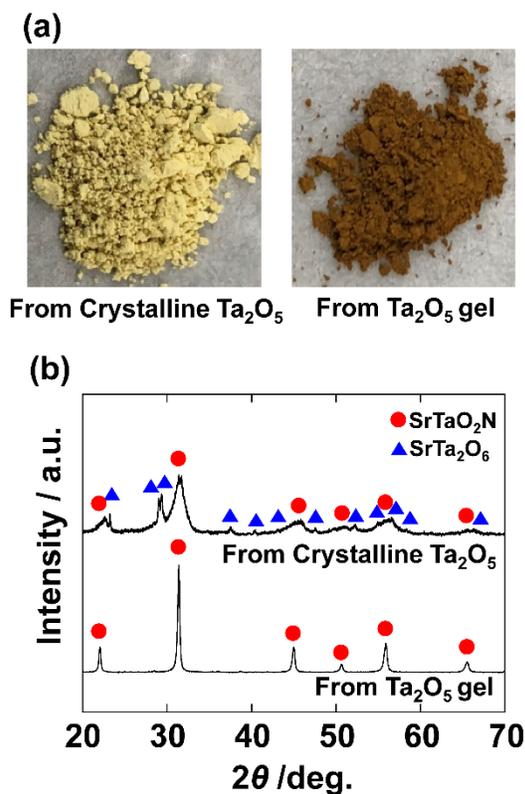

Figure 1. (a) Optical photographs and (b) XRD patterns of the products obtained from a mixture of $SrCO_3$, Ta_2O_5, and urea after heat treatment at 900 °C for 2 h. The molar ratio of $Sr/Ta/CO(NH_2)_2$ was 1:1:5. Both the Ta_2O_5 gel and crystalline Ta_2O_5 were examined.

diffraction peaks for $SrCO_3$ were observed and peaks for urea were not present. Only negligible changes in the XRD patterns were found for the mixture heat-treated at 500 °C compared with that heat-treated at 300 °C. Previously, we have reported on the preparation of $LaTiO_2N$ from a mixture of $La_2Ti_2O_7$ and $La(OH)_3$ via nitridation using urea.[49] In this previous research, the formation of $La_2O_2CN_2$ was initiated during the reaction between $La(OH)_3$ and urea at temperatures between 100 °C and 200 °C. In the current synthetic process for $SrTaO_2N$, formation of $SrCN_2$ was not observed at temperatures less than 500 °C. For the sample heat-treated at 700 °C, diffraction peaks attributed to $SrCN_2$ and $SrTaON_2$ were observed. This suggests that C–N species similar to biuret, cyanuric acid, melamine, and melamine condensation products (e.g., melam, melem, and melon) exist in an amorphous state as the thermolysis products of urea at moderate temperatures of less than 500 °C.[57] When the temperature was increased above 500 °C, $SrCN_2$ was generated by reaction of $SrCO_3$ with these thermolysis of products of urea. Finally, formation of $SrTaO_2N$ was initiated between 500 °C and 700 °C. New diffraction peaks for Ta_3N_5 were also found in addition to those of $SrCN_2$ and $SrTaO_2N$ in the pattern of the sample heat-treated at 800 °C. When the mixtures were heated at 900 °C, diffraction peaks for $SrCN_2$ and Ta_3N_5 were not present and strong diffraction peaks for $SrTaO_2N$ were observed. The intensities of the diffraction peaks for $SrTaO_2N$ increased with increases in the TaN were observed, they are negligible. The optimum
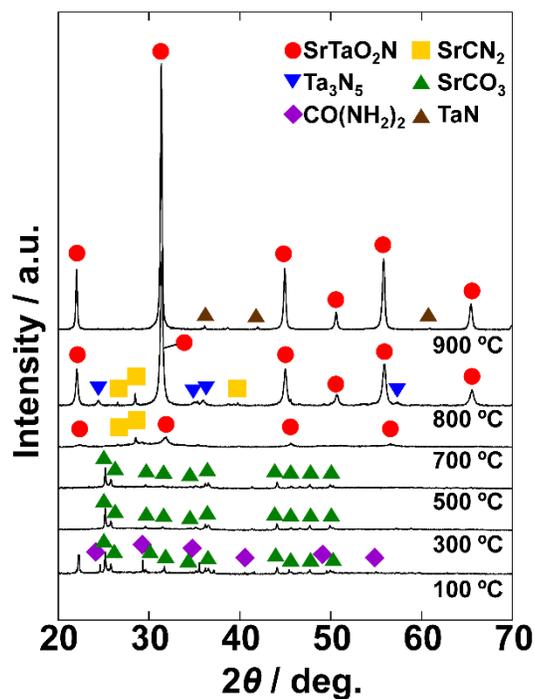
Figure 2. XRD patterns of the products obtained from a mixture of $SrCO_3$, Ta_2O_5 gel, and urea after heat treatment at various temperatures for 2 h. The molar ratio of $Sr/Ta/CO(NH_2)_2$ was 1:1:5.
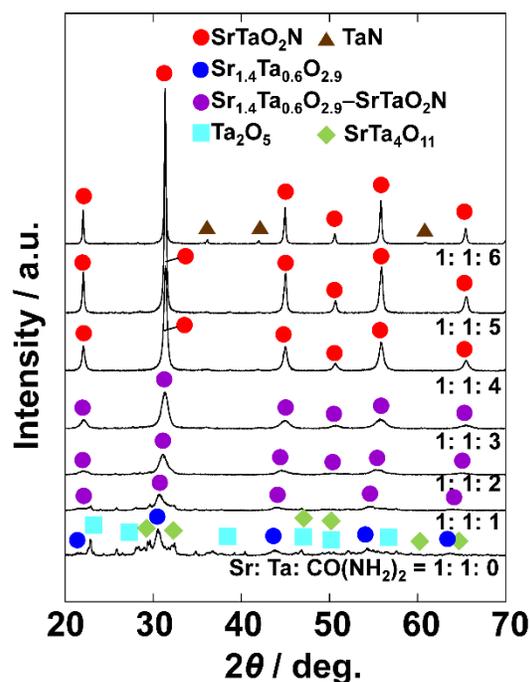

Figure 3. XRD patterns of products obtained from mixtures of $SrCO_3$, Ta_2O_5 gel, and urea after heat treatment at 900 °C for 2 h. The molar ratios of $Sr/Ta/CO(NH_2)_2$ were 1:1:0, 1:1:1, 1:1:2, 1:1:3, 1:1:4, 1:1:5, and 1:1:6.

calcination temperature was 900 °C, which is lower than the temperature typically required for synthesis of $SrTaO_2N$ via ammonolysis. More importantly, the calcination period, 2 h, is also extremely shorter than that required for ammonolysis (Table S1). It indicates that the energy consumption in our system is lower than previous systems. Though another solid-state nitriding agent, C_3N_4, achieves much lower heat-treatment temperature,[47] it requires an additional energy consumption for synthesis of C_3N_4. Therefore, the current system is environmentally-benign not only in that it does not requires toxic elements and gas, but also in that it reduces energy consumption during synthesis. We used this temperature, 900 °C, in subsequent experiments. SEM observations given in Figure S2 revealed that the products have indefinite shapes. The image for the sample heat-treated at 100 °C shows the micrometer sized grains. On the other hand, the primary particles with the diameter ≤100 nm are found for the image of the sample heat-treated at 900 °C. It suggests that the amorphous gels crystallized as nanosized primary particles during the nitriding process.

The amount of urea should affect the degree of nitridation of the resultant strontium–tantalum oxynitrides. We investigated the effect of the molar ratios of urea to $SrCO_3$ and Ta_2O_5 gel. First, the molar ratio (x:y) of Sr and Ta in the starting mixture was fixed at 1:1 and the urea molar ratio (z) was varied from 0 to 6. The calcination period and temperature were fixed at 2 h and 900 °C, respectively. Figure 3 shows the XRD patterns of the products obtained after calcination of mixtures of $SrCO_3$, Ta_2O_5, and urea with various molar ratios. When the calcination was carried out without urea (i.e., z = 0), crystalline phases of oxides, such as Ta_2O_5 and $SrTa_4O_{11}$, were observed

in the XRD pattern. In addition, broad diffraction peaks resembling perovskite-like phases were also present in the XRD pattern. Because there was no nitriding agent (i.e., urea), these peaks were not for the perovskite-type oxynitride, $SrTaO_2N$. Deniard and co-workers reported a perovskite-like strontium–tantalum oxide, $Sr_{1.4}Ta_{0.6}O_{2.9}$, where a certain amount of Sr substituted Ta in the *B* sites of the oxygen-deficient perovskite structure.[58] The lattice constant calculated from the peaks of the perovskite-like phase in the pattern (a = 8.264(3) Å, cubic approximation) corresponded to that of $Sr_{1.4}Ta_{0.6}O_{2.9}$ (a = 8.2768(1) Å) reported in the literature.[58] For the products prepared using mixtures with high urea molar ratios (i.e., z ≥ 5), sharp diffraction peaks attributable to the perovskite phase were observed in the XRD patterns. The lattice constants calculated from these peaks almost corresponded to that of $SrTaO_2N$ (Table S2). In addition, peaks for TaN were confirmed in the sample synthesized with a urea molar ratio of z = 6. This suggested that addition of excessive urea caused contamination with metal nitride as a by-product. The XRD patterns of samples obtained from mixtures with z = 1, 2, and 3 showed that the products contained a single perovskite phase. The peak positions lay between those of $Sr_{1.4}Ta_{0.6}O_{2.9}$ and $SrTaO_2N$. The lattice constants of these products were also between those of $Sr_{1.4}Ta_{0.6}O_{2.9}$ and $SrTaO_2N$ (Tables S2 and S3). These results suggested that the obtained products were the Sr-Ta perovskite oxynitrides as solid solutions of $Sr_{1.4}Ta_{0.6}O_{2.9}$ and $SrTaO_2N$. When the urea molar ratio (z) increased, the diffraction peaks shifted in the wide-angle direction, approaching the peak positions for $SrTaO_2N$. Accordingly, as the amount of urea increased, the ratio of Sr

Table 1. Oxygen and nitrogen contents of the products prepared from mixtures of $SrCO_3$, Ta_2O_5, and urea with various molar ratios after heat treatment at 900 °C for 2 h

Molar ratio of Sr:Ta:CO(NH₂)₂	O (wt%)	N (wt%)	O/N weight ratio	O/N molar ratio
1: 1: 1	14.5(1)	–	–	–
1: 1: 2	13.3(5)	0.799(1)	16.7	14.6
1: 1: 3	12.9(2)	1.64(1)	7.90	6.92
1: 1: 4	11.4(1)	2.46(8)	4.64	4.06
1: 1: 5	9.93(2)	3.53(2)	2.82	2.46

decreased and that of Ta increased and the ratio of Sr:Ta approached 1:1. The elemental compositions of the products were investigated using O/N combustion analysis and ICP-OES. Table 1 summarizes the oxygen and nitrogen contents of the products prepared from the mixtures of $SrCO_3$, Ta_2O_5, and urea with various molar ratios. The nitrogen concentration in the products increased and the O/N molar ratio decreased with increases in the amount of urea. When the molar ratio of Sr:Ta:urea in the precursor mixture was 1:1:5, the O/N molar ratio of the product was 2.46, which was relatively close to the theoretical ratio of O/N in $SrTaO_2N$. The deviation from the ideal ratio (O/N = 2) is considered to be due to the reduction of Ta^{5+} to Ta^{4+} (See the discussion later for details). For the samples prepared from mixtures with $Sr/Ta/CO(NH_2)_2$ molar ratios of 1:1:2, 1:1:3, and 1:1:4, there was an excess of oxygen in the products compared with nitrogen. The ICP-OES measurements revealed that the molar ratio of the cations (i.e., Sr and Ta) in the products was approximately 1:1 in all cases (Table S4). This suggests that volatilization of the metals does not occur and the metal composition of the products is maintained at the original value of the precursors even after the calcination process. Therefore, the obtained products contain amorphous Ta oxides in addition to the perovskite solid solution.

Next, we studied the effect of the amount of urea in the precursor on the color properties of the prepared Sr-Ta perovskite oxynitride solid solutions. Optical photographs and UV-Vis diffuse reflectance spectra of the products are shown in Figure 4. The product prepared from the mixture with a low urea molar ratio ($z = 1$) was almost colorless (Figure 4a). This product showed high reflectance in the visible region from 400 to 800 nm in the UV-Vis diffuse reflectance spectrum (Figure 4b). Because this product was a mixture of metal oxides and did not contain nitrogen as anion, its band gap was wide because the band gap width is directly related to the O $2p$ levels and Ta $5d$ levels. By contrast, the products prepared from mixtures with higher urea molar ratios ($z \geq 2$) exhibited chromatic colors. These samples contained a certain amount of nitrogen as an anion, so their band gaps were narrower than those of the oxides because of the presence of N $2p$ states above the O $2p$ state in their valence bands.[31,34] This enabled absorption of visible light. The valence band edge is very sensitive to changes in the O/N ratio.[59] As shown in Figure S3, if the products were mixtures of $Sr_{1.4}Ta_{0.6}O_{2.9}$ and $SrTaO_2N$, the
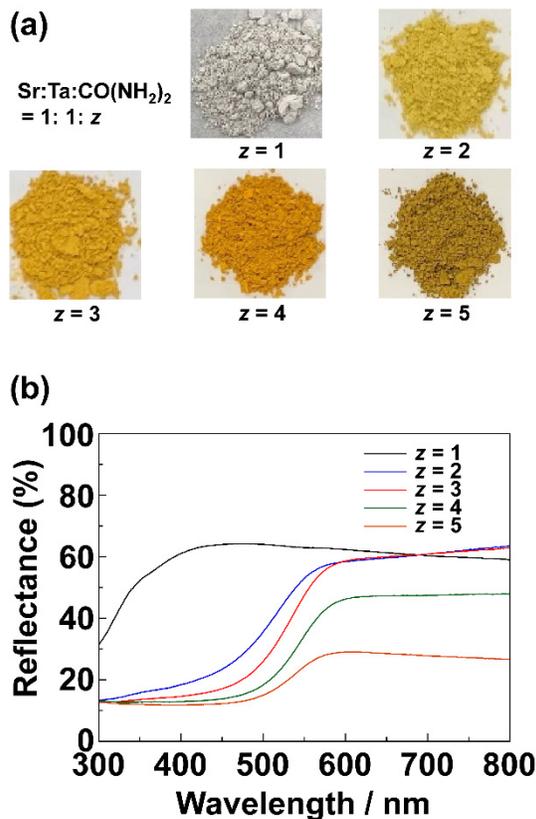

(a) Sr:Ta:CO(NH₂)₂ = 1: 1: z

z = 1   z = 2   z = 3   z = 4   z = 5

(b)

Figure 4. (a) Optical photographs and (b) UV-Vis diffuse reflectance spectra of the products obtained from mixtures of $SrCO_3$, Ta_2O_5, and urea after heat treatment at 900 °C for 2 h. The molar ratios of $Sr/Ta/CO(NH_2)_2$ were 1:1:1, 1:1:2, 1:1:3, 1:1:4, and 1:1:5.

UV-Vis diffuse reflectance spectrum shows the 2-step adsorption edges based on the band gaps of each compound. Therefore, these spectra also strongly support the formation of solid solutions. A progressive decrease in the O/N ratio, that is, an increase in the nitrogen content, in the oxynitride solid solutions induced a continuous shift in the absorption edge from 520 nm to 560 nm. The increase in the nitrogen content of the oxynitride solid solutions resulted in a decrease in the maximum intensity of reflectance as well as the red shifts of the absorption edge. These results corresponded to the change in the color of product from yellow to brown (Figure 4a). The CIE-$L*a*b*Ch°$ color coordinates and bandgap energy (E_g) values of the products are summarized in Table 2. The E_g values of the products were estimated using the following conventional equation:[60]

$$E_g \text{ (eV)} = 1240/\lambda \text{ (nm)}$$

where λ represents the absorption edge of the absorption spectra processed using the Kubelka–Munk function (Figure S4). The product prepared with $z = 1$ had a wide band gap (E_g = 3.65 eV). On the other hand, the band gap of the product prepared with $z = 5$ is narrow (E_g = 2.21 eV). This E_g value is comparable to that of $SrTaO_2N$ prepared via ammonolysis (E_g

Table 2. Color coordinates and band gap energies (E_g) of the products obtained from mixtures of $SrCO_3$, Ta_2O_5, and urea after heat treatment at 900 °C for 2 h. The molar ratios of Sr/Ta/CO(NH$_2$)$_2$ were 1:1:1, 1:1:2, 1:1:3, 1:1:4, and 1:1:5

Molar ratio of Sr: Ta: CO(NH$_2$)$_2$	Color coordinates					E_g / eV
	L^*	a^*	b^*	C	$h°$	
1: 1: 1	87.8	−0.80	+1.02	1.30	128.1	3.65
1: 1: 2	73.9	−5.78	+38.1	38.5	98.6	2.38
1: 1: 3	72.2	−4.76	+43.7	44.0	96.2	2.34
1: 1: 4	66.8	+9.19	+56.4	57.1	80.7	2.25
1: 1: 5	47.1	+5.92	+43.8	44.2	82.3	2.21

= 2.1 eV)[31]. For the product prepared with $z = 1$, the values of a^* and b^* were close to 0 and the L^* value was relatively high. Consequently, it appeared almost white, in good agreement with the wide band gap. With increases in the amount of nitrogen in the solid solutions, the a* and b* values increased and the L^* value decreased. The value of $h°$ was between 70° and 105°, indicating that the hue was yellow. Larger C values indicated a more chromatic or saturated color. Chroma is also related to the cleanliness of a color. The incorporation of nitrogen as an anion improved the chroma, especially in the case of $z = 4$, which had the highest C value (57.1). The a^*, b^*, and C values for the product with $z = 5$ were lower than those for the product with $z = 4$, though the E_g value of the product with $z = 5$ was smaller than that of the product $z = 4$. These results could be attributed to lower reflectance of the $z = 5$ product compared with that of the $z = 4$ product over the entire wavelength region (Figure 4b and Figure S3). Urea acts both as a nitriding agent and a reducing agent.[61] Therefore, reduction of cations, for example, from Ta^{5+} to Ta^{4+}. The lower reflectance (Figure 4b), or background absorption (Figure S4), observed in the longer wavelength region could be attributed to these reduced cationic species. Therefore, the C value of the product with $z = 5$ is lower than those of the product with $z = 4$.
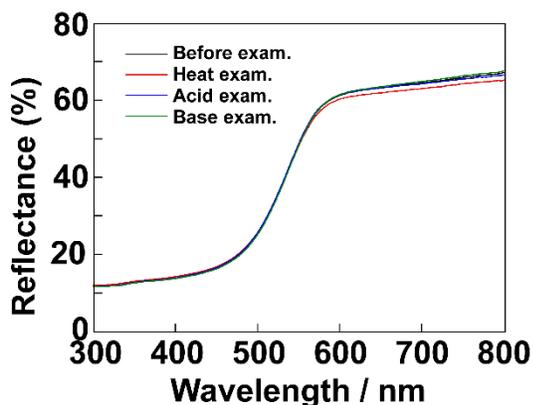
Finally, the thermal and chemical stabilities of the products were evaluated. The product with $z = 3$ was used as an example. To evaluate the thermal stability, i.e., heat examination, the sample was heated in a crucible at 400 °C for 5 h in air and cooled to room temperature. The chemical stabilities, i.e., acid and base resistance examination, of the sample was evaluated using aqueous solutions of 4 % acetic acid and 4 % ammonium bicarbonate. The product was dispersed into the solutions and incubated at room temperature for 24 h. Then, the samples were rinsed with deionized water and EtOH, and dried at room temperature. The color of the samples after the heat, acid, and base resistant examinations evaluated by UV-Vis diffuse reflectance spectra and color coordinate data. Figure 5 shows UV-Vis diffuse reflectance spectra of the product measured before and after the heat, acid, and base resistant examinations. The changes in spectral shape after each resistance test are negligible. The color coordinate data were examined and the color difference (ΔE) was estimated from the color coordinate data before and after the examinations using the following equation[16]:

$$\Delta E = [(L^*_{after} - L^*_{before})^2 + (a^*_{after} - a^*_{before})^2 + (b^*_{after} - b^*_{before})^2]^{1/2}$$

The color coordinate data of the samples before and after the heat, acid, and base resistant examinations are summarized in Table S5. ΔE values for after heat, acid, and base resistant examinations are 3.4, 4.1, and 4.3, respectively. These small ΔE values are negligible and indicate that the color of the product is stable and it is clear that the products possesses high thermal and chemical stabilities. Therefore, it is evident that strontium–tantalum perovskite oxynitrides solid solutions prepared using urea have enough potentials for environmentally-benign alternatives to conventional pigments containing heavy metals .

Figure 5. UV-Vis diffuse reflectance spectra of the products obtained from a mixture of $SrCO_3$, Ta_2O_5 gel, and urea after heat treatment at 900 °C for 2 h. The molar ratio of Sr/Ta/CO(NH$_2$)$_2$ was 1:1:3. The spectra were measured before and after heat, acid, and base resistant examinations.

CONCLUSIONS

We have successfully developed a facile synthetic procedure to prepare strontium–tantalum perovskite oxynitrides. This method uses urea as a solid-state nitriding agent instead of gaseous NH$_3$. Ta$_2$O$_5$ gel prepared by hydrolysis and condensation of Ta(OC$_2$H$_5$)$_5$ is suitable as a precursor for strontium–tantalum perovskite oxynitrides for the urea nitriding method. Strontium–tantalum oxynitride could be

prepared by heat-treatment of a mixture of $SrCO_3$, Ta_2O_5 gel, and urea under a flow of N_2 gas. This simple procedure is more suitable for the production of oxynitrides on a large scale than the conventional toxic ammonia nitriding method. The lower heat-treatment temperature and the shorter reaction time, i.e., the reduced energy consumption, compared with the ammonolysis method are also important advantages from the point of view of green chemistry. An oxynitride with an XRD pattern corresponding to that of $SrTaO_2N$ was obtained with a $Sr:Ta:CO(NH_2)_2$ precursor molar ratio of 1:1:5 after heat treatment at 900 °C. When the amount of urea in the precursor was reduced, the strontium–tantalum perovskite oxynitrides solid solutions of $Sr_{1.4}Ta_{0.6}O_{2.9}$ and $SrTaO_2N$ were obtained. The products exhibited optical absorption and chromatic colors because of the narrower band gaps of the oxynitrides compared with those of oxides. The O/N ratio can be easily adjusted by changing of the amount of urea in the precursor. As a result, the color of the product can be turned from yellow to brown. The synthetic strategy for preparation of strontium–tantalum perovskite oxynitrides solid solutions developed in this work could be used to synthesize potential candidate for use as environmentally-benign pigment alternatives to conventional inorganic pigments containing toxic elements.

ASSOCIATED CONTENT

Supporting Information

The Supporting Information is available free of charge at https://pubs.acs.org/doi/10.1021/acs.inorgchem.xxxxxxx.

Summary of syntheses of $SrTaO_2N$ from various precursors and nitriding agents (Table S1); XRD patterns of commercial Ta_2O_5 and sol-gel derived Ta_2O_5 gel (Figure S1); SEM images of the products (Figure S2); Lattice parameters of products obtained from mixtures of $SrCO_3$, Ta_2O_5 gel, and urea (Tables S2–S3); Contents of Sr and Ta in the products determined by ICP-OES measurements of the products (Table S4); Kubelka–Munk transformed reflectance spectra of UV-Vis diffuse reflectance spectroscopy of the product and the mixture of $Sr_{1.4}Ta_{0.6}O_{2.9}$ and $SrTaO_2N$ (Figure S3); Kubelka–Munk transformed reflectance spectra of UV-vis diffuse reflectance spectroscopy of the products obtained from precursors with various ratios (Figure S4); Color coordinates of the products before and after thermal, acid, and base resistant examinations (Table S5) (PDF)

AUTHOR INFORMATION

Corresponding Author

Kiyofumi Katagiri − *Graduate School of Advanced Science and Engineering, Hiroshima University, Higashi-Hiroshima 739-8527, Japan;* orcid.org/0000-0002-9548-9835; Email: kktgr@hiroshima-u.ac.jp

Authors

Takuya Sakata − *Graduate School of Advanced Science and Engineering, Hiroshima University, Higashi-Hiroshima 739-8527, Japan*

Western Region Industrial Research Center, Hiroshima Prefectural Technology Research Institute, 2-10-1 Aga-Minami, Kure 737-0004, Japan

Risa Yoshiyuki − *Graduate School of Advanced Science and Engineering, Hiroshima University, Higashi-Hiroshima 739-8527, Japan*

Ryoki Okada − *Graduate School of Advanced Science and Engineering, Hiroshima University, Higashi-Hiroshima 739-8527, Japan*

Sohta Urushidani − *Graduate School of Advanced Science and Engineering, Hiroshima University, Higashi-Hiroshima 739-8527, Japan*

Naoki Tarutani − *Graduate School of Advanced Science and Engineering, Hiroshima University, Higashi-Hiroshima 739-8527, Japan;* orcid.org/0000-0003-0696-8082

Kei Inumaru − *Graduate School of Advanced Science and Engineering, Hiroshima University, Higashi-Hiroshima 739-8527, Japan;* orcid.org/0000-0001-6876-3854

Kyohei Koyama − *Graduate School of Chemical Sciences and Engineering, Hokkaido University, N13 W8, Kita-ku, Sapporo 060-8628, Japan*

Yuji Masubuchi − *Division of Applied Chemistry, Faculty of Engineering, Hokkaido University, N13 W8, Kita-ku, Sapporo 060-8628, Japan;* orcid.org/0000-0003-3601-7077

Complete contact information is available at:

https://pubs.acs.org/10.1021/acssuschemeng.9bxxxxx

Author Contributions

The manuscript was written through contributions of all authors. All authors have given approval to the final version of the manuscript.

Notes

The authors declare no competing financial interest. All data needed to evaluate the conclusions in the paper are present in the paper and/or the Supplementary Materials.

REFERENCES

(1) Nassau, K. *The Physics and Chemistry of Color: The Fifteen Causes of Color*; 2nd ed.; John Wiley & Sons, Inc.: New York, NY, 2001.

(2) Kuehni, R. G. *Color: An Introduction to Practice and Principles*; 2nd ed.; John Wiley & Sons, Inc.: Hoboken, NJ, 2005.

(3) Buxbaum, G.; Pfaff, G. *Industrial Inorganic Pigments*; 3rd ed.; Wiley-VCH: Weinheim, 2005.

(4) Faulkner, E. B.; Schwartz, R. J. *High Performance Pigments;* 2nd ed.; Wiley-VCH: Weinhein, 2009.

(5) Pan, Z.; Wang, Y.; Huang, H.; Ling, Z.; Dai, Y.; Ke, S. Recent Development on Preparation of Ceramic Inks in Ink-Jet Printing. *Ceram. Int.* **2015**, *41*, 12515–12528.

(6) Gilani, S. H.; Marano, M. Chromium Poisoning and Chick Embryogenesis. *Environ. Res.* **1979**, *19*, 427–431.

(7) Rustagi, N.; Singh, R. Mercury and Health Care. *Indian J. Occup. Environ. Med.* **2010**, *14*, 45–48.

(8) Rice, K. M.: Walker, E. M.: Wu, M.; Gillette, C.; Blough, E. R. Environmental Mercury and Its Toxic Effects. *J. Prev. Med. Public Health* **2014**, *47*, 74–83.

(9) Wani, A. L.; Ara, A.; Usmani, J. A. Lead Toxicity: A Review. *Interdiscip. Toxicol.* **2015**, *8*, 55–64.

(10) E.U. Parliament. EU Council. Directive 2002/95/EC of the European Parliament and of the Council on the Restriction of the Use of Certain Hazardous Substances in Electrical and Electronic Equipment. *Off. J. Eur. Union* **2003**, *46*, 19–23.

(11) Jansen, M.; Letschert, H. P. Inorganic Yellow-Red Pigments without Toxic Metals. *Nature* **2000**, *404*, 980–982.

(12) García, A.; Llusar, M.; Calbo, J.; Tena, M. A.; Monrós, G. Low-Toxicity Red Ceramic Pigments for Porcelainised Stoneware from Lanthanide–Cerianite Solid Solutions. *Green Chem.* **2001**, *3*, 238–242.

(13) Sreeram, K. J.; Srinivasan, R.; Devi, J. M.; Nair, B. U.; Ramasami, T. Cerium Molybdenum Oxides for Environmentally Benign Pigments. *Dyes Pigm.* **2007**, *75*, 687–692.

(14) Vishnu, V. S.; Jose, S.; Reddy, M. L. Novel Environmentally Benign Yellow Inorganic Pigments Based on Solid Solutions of Samarium–Transition Metal Mixed Oxides. *J. Am. Ceram. Soc.* **2011**, *94*, 997–1001.

(15) Radhika, S. P.; Sreeram, K. J.; Nair, B. U. Mo-Doped Cerium Gadolinium Oxide as Environmentally Sustainable Yellow Pigments. *ACS Sustainable Chem. Eng.* **2014**, *2*, 1251–1256.

(16) Wendusu, Shiraishi, A.; Takeuchi, N.; Masui, T.; Imanaka, N. Novel Environment Friendly Inorganic Red Pigments Based on $Bi_4V_2O_{11}$. *RSC Adv.* **2015**, *5*, 44886–44894.

(17) Oka, R.; Shobu, Y.; Aoyama, F.; Tsukimori, T.; Masui, T. Synthesis and Characterisation of $SrY_{2-x}Ce_xO_4$ as Environmentally Friendly Reddish-Brown Pigments. *RSC Adv.* **2017**, *7*, 55081–55087.

(18) Huang, B.; Xiao, Y.; Zhou, H.; Chen, J.; Sun, X. Synthesis and Characterization of Yellow Pigments of $Bi_{1.7}RE_{0.3}W_{0.7}Mo_{0.3}O_6$ (RE = Y, Yb, Gd, Lu) with High NIR Reflectance. *ACS Sustainable Chem. Eng.* **2018**, *6*, 10735–10741.

(19) Raj, A. K. V.; Rao, P. P.; Sreena, T. S. Color Tunable Pigments with High NIR Reflectance in Terbium-Doped Cerate Systems for Sustainable Energy Saving Applications. *ACS Sustainable Chem. Eng.* **2019**, *7*, 8804–8815.

(20) Maeda, K.; Teramura, K.; Lu, D.; Takata, T.; Saito, N.; Inoue, Y.; Domen, K. Photocatalyst Releasing Hydrogen from Water. *Nature* **2006**, *440*, 295.

(21) Fuertes, A. Metal Oxynitrides as Emerging Materials with Photocatalytic and Electronic Properties. *Mater. Horiz.* **2015**, *2*, 453–461.

(22) Maeda, K.; Domen, K. Development of Novel Photocatalyst and Cocatalyst Materials for Water Splitting under Visible Light. *Bull. Chem. Soc. Jpn.* **2016**, *89*, 627–648.

(23) Xie, R. J.; Hirosaki, N. Silicon-Based Oxynitride and Nitride Phosphors for White LEDs—A Review. *Sci. Technol. Adv. Mater.* **2007**, *8*, 588–600.

(24) Ogi, T.; Iwasaki, H.; Nandiyanto, A. B. D.; Iskandar, F.; Wang, W. N.; Okuyama, K. Direct White Light Emission from a Rare-Earth-Free Aluminium–Boron–Carbon–Oxynitride Phosphor. *J. Mater. Chem. C* **2014**, *2*, 4297–4303.

(25) Yang, M.; Oró-Solé, J.; Kusmartseva, A.; Fuertes, A.; Attfield, J. P. Electronic Tuning of Two Metals and Colossal Magnetoresistances in $EuWO_{1+x}N_{2-x}$ Perovskites. *J. Am. Chem. Soc.* **2010**, *132*, 4822–4829.

(26) Kim, Y. I.; Woodward, P. M.; Baba-Kishi, K. Z.; Tai, C. W. Characterization of the Structural, Optical, and Dielectric Properties of Oxynitride Perovskites AMO_2N (A = Ba, Sr, Ca; M = Ta, Nb). *Chem. Mater.* **2004**, *16*, 1267–1276.

(27) Lu, H. H.; Xu, J. P.; Liu, L.; Wang, L. S.; Lai, P. T.; Tang, W. M. Improved Interfacial Quality of GaAs Metal-Oxide-Semiconductor Device with NH_3-Plasma Treated Yittrium-Oxynitride as Interfacial Passivation Layer. *Microelectron. Reliab.* **2016**, *56*, 17–21.

(28) Cheviré, F.; Tessier, F.; Marchand, R. Optical Properties of the Perovskite Solid Solution $LaTiO_2N–ATiO_3$(A = Sr, Ba). *Eur. J. Inorg. Chem.* **2006**, *2006*, 1223–1230.

(29) Pastrana-Fábregas, R.; Isasi-Marín, J.; Sáez-Puche, R. Synthesis and Characterization of Inorganic Pigments Based on Transition Metal Oxynitrides. *J. Mater. Res.* **2006**, *21*, 2255–2260.

(30) Aguiar, R.; Logvinovich, D.; Weidenkaff, A.; Rachel, A.; Reller, A.; Ebbinghaus, S. G. The Vast Colour Spectrum of Ternary Metal Oxynitride Pigments. *Dyes Pigm.* **2008**, *76*, 70–75.

(31) Xie, R. J.; Hintzen, H. T. Optical Properties of (Oxy)Nitride Materials: A Review. *J. Am. Ceram. Soc.* **2013**, *96*, 665–687.

(32) Ebbinghaus, S. G.; Abicht, H. P.; Dronskowski, R.; Müller, T.; Reller, A.; Weidenkaff, A. Perovskite-Related Oxynitrides – Recent Developments in Synthesis, Characterisation and Investigations of Physical Properties. *Prog. Solid State Chem.* **2009**, *37*, 173–205.

(33) Moon, K.-H.; Kim, J.-M.; Sohn, Y.; Cho, D. W.; Kim, Y.-I.; Avdeev, M. Crystal Structures and Color Properties of New Complex Perovskite Oxynitrides $AMg_{0.2}Ta_{0.8}O_{2.6}N_{0.4}$ (A = Sr, Ba). *Dalton Trans.* **2016**, *45*, 5614–5621.

(34) Tessier, F.; Maillard, P.; Cheviré, F.; Domen, K.; Kikkawa, S. Optical Properties of Oxynitride Powders. *J. Ceram. Soc. Jpn.* **2009**, *117*, 1–5.

(35) Fuertes, A. Nitride Tuning of Transition Metal Perovskites. *APL Mater.* **2020**, *8*, 020903.

(36) Kasahara, A.; Nukumizu, K.; Hitoki, G.; Takata, T.; Kondo, J. N.; Hara, M.; Kobayashi, H.; Domen, K. Photoreactions on $LaTiO_2N$ under Visible Light Irradiation. *J. Phys. Chem. A* **2002**, *106*, 6750–6753.

(37) Maillard, P.; Tessier, F.; Orhan, E.; Cheviré, F.; Marchand, R. Thermal Ammonolysis Study of the Rare-Earth Tantalates $RTaO_4$. *Chem. Mater.* **2005**, *17*, 152–156.

(38) Fuertes, A. Chemistry and Applications of Oxynitride Perovskites. *J. Mater. Chem.* **2012**, *22*, 3293–3299.

(39) Miura, A.; Takei, T.; Kumada, N. Synthesis of Wurtzite-Type InN Crystals by Low-Temperature Nitridation of $LiInO_2$ Using $NaNH_2$ Flux. *Cryst. Growth Des.* **2012**, *12*, 4545–4547.

(40) Miura, A.; Rosero-Navarro, C.; Masubuchi, Y.; Higuchi, M.; Kikkawa, S.; Tadanaga, K. Nitrogen-Rich Manganese Oxynitrides with Enhanced Catalytic Activity in the Oxygen Reduction Reaction. *Angew. Chem. Int. Ed.* **2016**, *55*, 7963–7967.

(41) Setsuda, Y.; Maruyama, Y.; Izawa, C.; Watanabe, T. Low-temperature Synthesis of $BaTaO_2N$ via the Flux Method Using $NaNH_2$. *Chem. Lett.* **2017**, *46*, 987–989.

(42) Odahara, J.; Miura, A.; Rosero-Navarro, N. C.; Tadanaga, K. Explosive Reaction for Barium Niobium Perovskite Oxynitride. *Inorg. Chem.* **2018**, *57*, 24–27.

(43) Sun, S.-K.; Motohashi, T.; Masubuchi, Y.; Kikkawa, S. Direct Synthesis of $SrTaO_2N$ from $SrCO_3/Ta_3N_5$ Involving CO Evolution. *J. Eur. Ceram. Soc.* **2014**, *34*, 4451–4455.

(44) Hosono, A.; Masubuchi, Y.; Yasui, S.; Takesada, M.; Endo, T.; Higuchi, M.; Itoh, M.; Kikkawa, S. Ferroelectric $BaTaO_2N$ Crystals Grown in a $BaCN_2$ Flux. *Inorg. Chem.* **2019**, *58*, 16752–16760.

(45) Hosono, A.; Masubuchi, Y.; Endo, T.; Kikkawa, S. Molten $BaCN_2$ for the Sintering and Crystal Growth of Dielectric Oxynitride Perovskites $Sr_{1-x}Ba_xTaO_2N$ (x = 0.04–0.23). *Dalton Trans.* **2017**, *46*, 16837–16844.

(46) Chen S.-L.; Guo, W.-M.; Sun, S-K.; Masubuchi, Y.; Lv, M.; Lin, H.-T.; Wang, C.-Y. Direct synthesis of nearly single phase $SrTaO2N$ from $SrCO_3/TaN$, *Ceram. Int.* **2018**, *44*, 4504–4507.

(47) Masubuchi, Y.; Tadaki, M.; Kikkawa, S. Synthesis of the Perovskite $SrTaO_2N$ Using C_3N_4 for Both Reduction and Nitridation. *Chem. Lett.* **2018**, *47*, 31–33.

(48) Yang, Q.; Masubuchi, Y.; Higuchi, M. Synthesis of Perovskite-Type Oxynitrides $SrNb(O,N)_3$ and $CaTa(O,N)_3$ Using Carbon Nitride. *Ceram. Int.* **2020**, *46*, 13941–13944.

(49) Gao, Q.; Giordano, C.; Antonietti, M.; Controlled Synthesis of Tantalum Oxynitride and Nitride Nanoparticles. *Small* **2011**, *7*, 3334–3340.

(50) Gomathi, A.; Reshma, S.; Rao, C.N.R. A Simple Urea-Based Route to Ternary Metal Oxynitride Nanoparticles, *J. Solid State Chem.* **2009**, *182*, 72–76.

(51) Okada, R.; Katagiri, K.; Masubuchi, Y.; Inumaru, K. Preparation of $LaTiO_2N$ Using Hydrothermally Synthesized $La_2Ti_2O_7$ as a Precursor and Urea as a Nitriding Agent. *Eur. J. Inorg. Chem.* **2019**, *2019*, 1257–1264.

(52) Katagiri, K.; Hayashi, Y.; Yoshiyuki, R.; Inumaru, K.; Uchiyama, T.; Nagata, N.; Uchimoto, Y.; Miyoshi, A.; Maeda, K. Mechanistic Insight on the Formation of GaN:ZnO Solid Solution from Zn-Ga Layered Double Hydroxide Using Urea as the Nitriding Agent. *Inorg. Chem.* **2018**, *57*, 13953–13962.

(53) Kim, N.; Stebbins, J. F. Structure of Amorphous Tantalum Oxide and Titania-Doped Tantala: ^{17}O NMR Results for Sol–Gel and Ion-Beam-Sputtered Materials. *Chem. Mater.* **2011**, *23*, 3460–3465.

(54) Kubelka, P.; Munk, F. Ein Beitrag Zur Optik Der Farbanstriche. F. *Z. Technol. Phys.* **1931**, *12*, 593–601.

(55) Völz, H. G. *Industrial Color Testing;* 2nd ed.; Wiley-VCH: Weinhein, 2002.

(56) Podsiadło, S. Stages of the Synthesis of Gallium Nitride with the Use of Urea. *Thermochim*. *Acta* **1995**, *256*, 367–373.

(57) Wirnhier, E.; Mesch, M. B.; Senker, J.; Schnick, W. Formation and Characterization of Melam, Melam Hydrate, and a Melam–Melem Adduct. *Chem. Eur. J.* **2013**, *19*, 2041–2049.

(58) Deniard, P.; Caldes, M. T.; Zou, X. D.; Diot, N.; Marchand, R.; Brec, R. Structural Modulation in $Sr_{1.4}Ta_{0.6}O_{2.9}$: Non-Harmonicity on ADPs During Rietveld Refinement. *Int. J. Inorg. Mater.* **2001**, *3*, 1121–1123.

(59) Widenmeyer, M.; Kohler, T.; Samolis, M.; De Denko, A. T.; Xiao, X.; Xie, W.; Osterloh, F. E.; Weidenkaff, A. Band Gap Adjustment in Perovskite-type $Eu_{1-x}Ca_xTiO_3$ via Ammonolysis. *Z. Phys. Chem.* **2020**, *234*, 887–909.

(60) Kudo, A.; Miseki, Y. Heterogeneous Photocatalyst Materials for Water Splitting. *Chem. Soc. Rev.* **2009**, *38*, 253–278.

(61) Lei, Z.; Lu, L.; Zhao, X. S. The Electrocapacitive Properties of Graphene Oxide Reduced by Urea. *Energy Environ. Sci.* **2012**, *5*, 6391–6399.

Table of Contents

Artwork
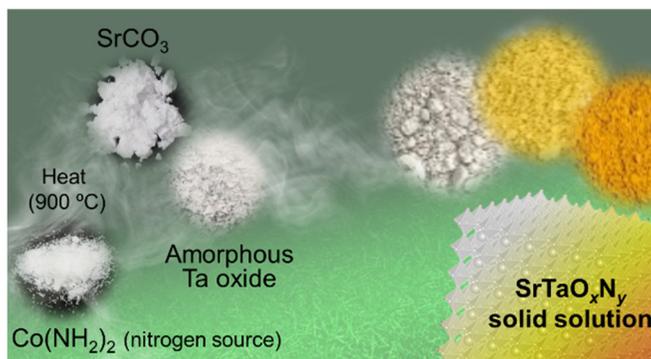
Synopsis text

Strontium–tantalum perovskite oxynitride and its solid solutions were prepared without ammonolysis. Urea was employed as a solid nitriding agent to eliminate the use of gaseous NH_3. The energy consumption can be reduced due to the shorter period and at the lower calcination temperature compared with the ammonolysis. The products exhibited chromatic colors because of the narrower band gaps of oxynitrides. The color the solid solutions were easily adjusted by varying the amount of urea.